Defense Technical Information Center Compilation Part Notice

ADP012239

TITLE: Studies of Intersubband Transitions in Arrays of Bi Nanowire Samples Using Optical Transmission

DISTRIBUTION: Approved for public release, distribution unlimited

This paper is part of the following report:

TITLE: Nanophase and Nanocomposite Materials IV held in Boston, Massachusetts on November 26-29, 2001

To order the complete compilation report, use: ADA401575

The following component part numbers comprise the compilation report:
ADP012174 thru ADP012259

Mat. Res. Soc. Symp. Proc. Vol. 703 © 2002 Materials Research Society V10.9

Studies of Intersubband Transitions in Arrays of Bi Nanowire Samples Using Optical Transmission

M. R. Black[a)], K. R. Maskaly[b)], O. Rabin[c)], Y. M. Lin[a)], S. B. Cronin[d)], M. Padi[d)], Y. Fink[b)], M. S. Dresselhaus[a,d)]
[a]Department of EECS, Massachusetts Institute of Technology, Cambridge, MA
[b]Department of Material Science and Engineering, Massachusetts Institute of Technology, Cambridge, MA
[c]Department of Chemistry, Massachusetts Institute of Technology, Cambridge, MA
[d]Department of Physics, Massachusetts Institute of Technology, Cambridge, MA

Abstract

This paper reports the fabrication of large diameter pores (> 150 nm) in anodic alumina that can be used to create wire arrays with significant surface effects, but without significant quantum confinement. These wires, therefore, allow us to distinguish between optical absorption spectra features originating from quantum effects and those from surface effects. The paper presents techniques towards fabricating these bismuth wire arrays, and presents optical absorption data from two bismuth nanowire arrays in the semimetal-semiconductor transition diameter regime. The results from previous publications are summarized and future directions are outlined.

Introduction

We are no longer completely limited to the constraints on the properties of 3D bulk materials. By utilizing quantum confinement, we have learned how to engineer the band gap of a material. As a result we can tailor the properties of a material to conform to a desired application. Once the effects of quantum confinement are fully understood, the size of the quantum confined dimension(s) can be selected to achieve the degree of quantum confinement and surface effects desired.

Bismuth nanowires exhibit a transition from a semimetal with a small band overlap (38 meV at 0 K) to a semiconductor, as the wire diameter becomes small enough to support significant quantum confinement effects, as shown in Fig. 1. This transition occurs in Bi nanowires at relatively large wire diameters because of its small effective masses and small band overlap. For example, this semimetal-semiconductor transition is predicted to occur at a wire diameter of 16 nm in the (012) direction (the growth direction of our nanowires) at room temperature, and at 47 nm at 77K, Fig. 1. The change from a semimetal to a semiconductor has significant effects on the electronic and optical properties of bismuth, which may be desirable for some applications, such as thermoelectricity.[1, 2]

We are working towards measuring the optical properties of bismuth wires in three different size regimes: large wire diameters (~ 200 nm) which are semimetals, small wire diameters (~ 15 nm) which are semiconductors, and an intermediate wire diameter size (~ 40 nm) where the wires are a semimetal at room temperature and a semiconductor at low temperatures. Well ordered arrays of 45 nm pores in alumina have been fabricated and filled with bismuth to create wires in the intermediate diameter regime. These wires are near the semimetal-semiconductor transition at 77K. The 45 nm wires absorb in the far infrared.

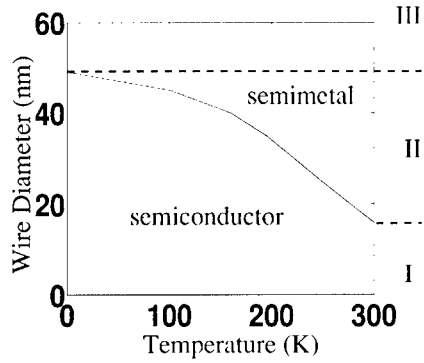

Figure 1: The phase diagram of the semimetal to semiconductor transition in bismuth nanowires is shown as a function of temperature and wire diameter. Depending on the wire diameter, a nanowire is either a semimetal (III), a semiconductor(I), or switches from a semimetal to a semiconductor as the temperature is decreased(II).

This optical absorption is attributed to intersubband transitions.[3] Well ordered arrays of small pore alumina templates (15 nm) have also been fabricated successfully. However, the liquid phase injection technique used to fill the alumina with bismuth is ineffective in filling these small diameter pores. We are therefore developing an electro-chemical method for filling small pores in anodic alumina with bismuth.[4] The process to fabricate the large pore alumina templates ($>$ 55 nm) proved to be the most difficult to develop due to the fact that the process requires a higher voltage and many highly sensitive process parameters needed to be optimized. Optical absorption measurements, like those already reported for 45 nm wires, for both the semiconducting and semimetallic wires will help us better understand the observed absorption spectra. We therefore seek to perform measurements over the whole diameter range to gain a better understanding of the quantum confinement characteristics of the Bi nanowires.

Fabrication and Experimental Details

Since aluminum can be anodized to form an alumina layer with an ordered array of pores[5], all the bismuth nanowires in this work were fabricated by filling porous anodic alumina. Several theories have been presented to explain the formation of the porous alumina, such as Refs. [5] and [6]. In addition, several theories have been recently proposed to explain the ordering of the pores into a hexagonal pattern when very specific conditions for the anodization are used.[7, 8] Many papers present excellent experimental results documenting conditions at which the anodization forms ordered pores and those at which the pores are irregular and not ordered.[9, 10, 11] However, to our knowledge, no complete theory exists to predict the optimal acid type, concentration, and temperature that should be used to obtain well-ordered arrays with a uniform pore diameter for a given anodization voltage and corresponding pore diameter. Therefore, whenever the desired pore size has not yet been well studied, many attempts of trial and error are required to establish the recipe for well-ordered

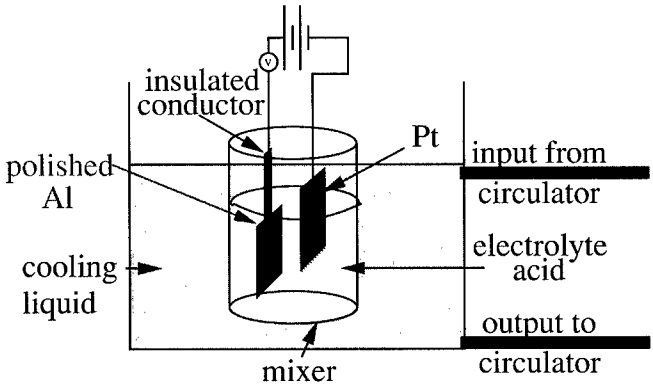

Figure 2: The anodization setup for high voltage anodization. The automatic cooling system, the high cooling liquid level, and the insulated conductor, all prevent breakdown during the anodization process.

pores. To minimize the trial and error required to find the ideal anodization conditions for large diameter pores (> 80 nm), we sought to reproduce the well-ordered arrays with a pore size of 200 nm diameter reported in Ref. [7]. However, when repeating their conditions of 160 V anodization voltage in 10 % phosphoric acid at 3°C, the anodization current became unstable. The current increased during the anodization, increasing the temperature of the acid. The rise in temperature in turn further increased the current, until the reaction became uncontrollable. This rapid rise in acid temperature and anodization current is called "breakdown" in the literature. [8]

In our samples, in addition to the increase in current at breakdown, sizzling occurred at the air/acid interface where the aluminum was exposed to air. Furthermore, the onset of this phenomenon was correlated with the ambient air temperature. This suggests that the sizzling is caused by the higher temperature of the sample at the surface (surface heating). We therefore implemented three techniques to reduce surface heating and the likelihood of breakdown, (see Fig. 2). When all three techniques are used, sizzling under our anodization conditions is eliminated. The first improvement was an automatic cooling system. A refrigerated recirculator is used to keep the cooling liquid at $-1.5 \pm 0.05\,^{\circ}\mathrm{C}$. In addition, the acid level is kept below that of the cooling liquid. This helps cool the air around the acid-air interface. Thirdly, the aluminum electrode is completely submerged in the chilled acid. In order to prevent shorting of the contact to the acid, an insulated conductor is used to make contact with the Al sheet inside the acid. The aluminum is anodized using this method for about 3 hours. The alumina is then etched off and the remaining aluminum then undergoes a second anodization for about 4 hours. The pores from a 40 V and a 160 V anodization are shown in Fig. 3 A and B, respectively.

The pores in the alumina are filled with Bi using a pressure injection technique.[12] The alumina template is then etched off using a selective etch, leaving only bismuth wires

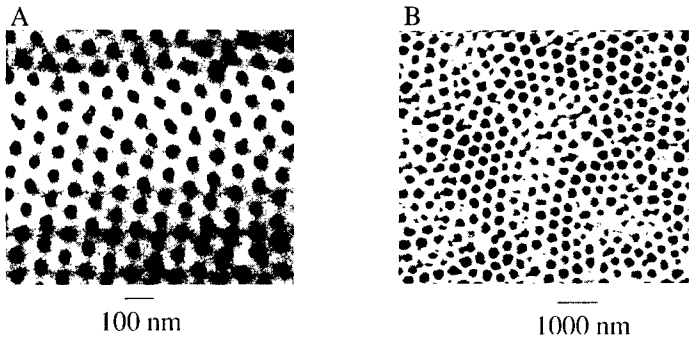

Figure 3: Scanning electron micrographs of anodic alumina anodized at (A) 40 V and (B) 160 V with pore diameters around 40 and 200 nm, respectively.

behind. Using the micro-FTIR (Fourier Transform Infrared Technique), the reflection and transmission were measured from free-standing Bi nanowires with a bismuth oxide coating around the nanowires and a thin Bi film holding them together. A schematic diagram of the sample is shown in Fig. 4(C). Bismuth nanowires protrude out of the bismuth film, which is balanced on the edge of a glass slide. Light is transmitted through the sample in the direction of the wires so that the electric field of the incident light is always perpendicular to the wire axis. Since the transmission is proportional to e^{-Kx}, where K is the infrared absorption coefficient and x is the sample thickness, the negative log of the transmission is proportional to the absorption coefficient. This is used to find the absorption spectra of the wires.

Results and Discussion

The absorption coefficients (times the sample thickness) as a function of wavenumber, obtained by taking the negative log of the transmission intensity of $\sim 45\,\text{nm}$ and $\sim 30\,\text{nm}$ diameter free-standing bismuth nanowires are shown in Fig. 4(A). For comparison, Fig. 4(A) also shows the absorption coefficient of a film of bismuth. The two arrays of wires used for the free-standing nanowire measurements had diameters of 60 nm and 45 nm before the alumina template surrounding the wires was etched away. Since a $\sim 7\,\text{nm}$ oxide grows on the free-standing wires after the alumina is selectively etched away [13], the inner bismuth portion of the free-standing wires is expected to have a diameter of around 45 nm and 30 nm. Since the thickness of the thin bismuth film holding the bismuth nanowires and the thickness of the nanowire array are not known, arbitrary units of absorption are used.

The absorption spectra of the nanowire arrays show many more features than that of the bismuth film. The absorption features are predominant for wavenumbers less than $1300\,cm^{-1}$. Simulations show that intersubband absorption tails off for $\omega > 1300\,cm^{-1}$ in bismuth nanowires, because of a fall off in the coupling between the initial and the final states.[14] Figure 4(A and B) also shows that the absorption spectra between the two wire arrays differ significantly. The absorption of each sample was taken several times and found

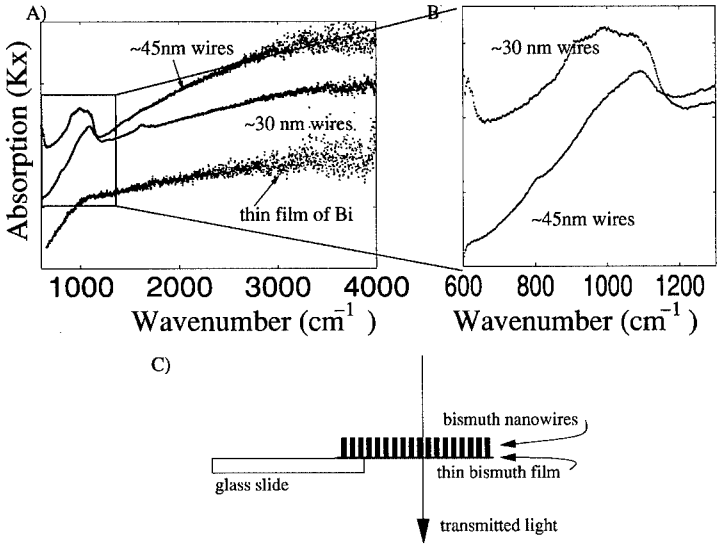

Figure 4: The dependence of the absorption coefficient on wavenumber, found by taking the negative log of the transmission of free-standing bismuth nanowires with diameters around 45 and 30 nm as well as the absorption on a thin piece of bismuth is shown in A) and B). C) shows a schematic of the experimental setup to measure absorption.

to be reproducible. The differences in the absorption spectra for wavenumbers less than $1300\,cm^{-1}$ are attributed to differences in the subband energies involved in intersubband absorption.[14]

Previous work on the optical properties of bismuth nanowire arrays inside the alumina template report a sharp absorption feature at about $1000\,cm^{-1}$.[3] The shape of the absorption peak, the frequency of observed absorption, the qualitative dependence on wire diameter, and the polarization of this absorption all indicate that intersubband transitions are the likely cause of the observed absorption.[3] In addition, a model for intersubband transitions in bismuth nanowires predicts peaks in the absorption spectra at energies that are in agreement with those observed in optical measurements of free standing wire arrays.[14] However, some aspects of the absorption curve remain unexplained. Firstly, although the energy of the absorption peak at around $1000\,cm^{-1}$ increases with decreasing wire diameter, as expected for intersubband transitions, it does not increase as rapidly as expected. Secondly, the relative intensities of the absorption peaks in the free standing wires are different from those predicted by theory.[14] In particular, the absorption peak at around $1000\,cm^{-1}$ is much more intense in the experimentally measured absorption than in the simulated intersubband absorption.[14] In this paper we report optical absorption measurements on $\sim$ 30 nm wires as well as the fabrication of ordered 200 nm pores in alumina. With the newly developed ability to fabricate well ordered 200 nm wire arrays and with the currently developing ability

to electro-chemically fill the 20 nm arrays, we hope to develop a better understanding of the observed absorption mechanisms in bismuth nanowire arrays.

Acknowledgements

The authors gratefully acknowledge the valuable discussions with of Prof. Jackie Ying and Dr. Gene Dresselhaus. The authors also gratefully acknowledge MURI subcontract 0205-G-BB953, NSF grant DMR-0116042, and US Navy contract N00167-98-0024 for support. This work made use of MRSEC Shared Facilities supported by the National Science Foundation contract DMR-9400334.

References

[1] Z. Zhang, X. Sun, M. S. Dresselhaus, J. Y. Ying, and J. Heremans, Phys. Rev. B **61**, 4850–4861 (2000).

[2] X. Sun, Z. Zhang, and M. S. Dresselhaus, Appl. Phys. Lett. **74**, 4005–4007 (1999).

[3] M. R. Black, M. Padi, S. B. Cronin, Y.-M. Lin, O. Rabin, T. McClure, G. Dresselhaus, P. L. Hagelstein, and M. S. Dresselhaus, Appl. Phys. Lett. **77**, 4142–4144 (2000).

[4] O. Rabin, Y. Lin, S. Cronin, and M. S. Dresselhaus. to be published.

[5] J. P. Sullivan and G. C. Wood, Proc. Roy Soc. Lond. A. **317**, 511–543 (1970).

[6] Feiyue Li, Lan Zhang, and Robert M. Metzger, Chem. Mater. **10**, 2470–2480 (1998).

[7] A. P. Li, F. Muller, A. Birner, K. Nielsch, and U. Gosele, Journal of Applied Physics **84**, 6023–6026 (1998).

[8] A. Jagminas, D. Bigelience, I. Mikulskas, and R. Tomasiunas, Journal of Crystal Growth **223**, 591–598 (2001).

[9] Hideki Masuda and Kenji Fukuda, Science **268**, 1466–1468 (1995).

[10] Y. Li, E. R. Holland, and P. R. Wilshaw, J. Vac. Sci. Technol. B. **18**, 994–996 (2000).

[11] T. E. Huber, M. J. Graf, C. A. Foss Jr., and P. Constant, J. Mater Res. **15**, 1816–1821 (2000).

[12] Z. Zhang, J. Ying, and M. Dresselhaus, J. Mater. Res. **13**, 1745–1748 (1998).

[13] S. B. Cronin, Y.-M. Lin, P. L. Gai, O. Rabin, M. R. Black, G. Dresselhaus, and M. S. Dresselhaus. In *Anisotropic Nanoparticles: Synthesis, Characterization and Applications: MRS Symposium Proceedings, Boston, December 2000*, edited by S. Stranick, P. C. Searson, L. A. Lyon, and C. Keating, pages C571–C576, Materials Research Society Press, Pittsburgh, PA, 2001. pdf.

[14] M. R. Black, Y. M. Lin, S. B. Cronin, O. Rabin, and M. S. Dresselhaus, unpublished.